

UDC 624.04.012.4.044, 519.853

## SEARCHING FOR A COMPROMISE SOLUTION IN CROSS-SECTION SIZE OPTIMIZATION PROBLEMS OF COLD-FORMED STEEL STRUCTURAL MEMBERS

V.V. Yurchenko<sup>1</sup>,

Doctor of Technical Science, Professor

I.D. Peleshko<sup>2</sup>,

Candidate of Technical Science, Associate Professor

<sup>1</sup>*Kyiv National University of Construction and Architecture  
Povitroflotskyj av., 31, Kyiv, 03680*

<sup>2</sup>*Lviv Polytechnic National University  
St. Bandery, 12, Lviv, 79013*

DOI: 10.32347/2410-2547.2022.109.72-92

A parametric optimization problem of cross-sectional sizes for cold-formed steel lipped channel structural members subjected to axial compression has been considered by the paper. An optimization problem is formulated as to define optimum cross-sectional sizes of cold-formed structural member taking into account post-buckling behavior (web and flange local and distortional buckling) of the member as well as structural requirements when the profile perimeter (strip width), profile thickness, design lengths of the structural member as well as material properties are constant and specified in advance. Maximization of the load-carrying capacity of the cold-formed structural member has been assumed as purpose function. The formulated parametric optimization problem has been solved by exhaustive search method using the software written in Python. As optimization results the cold-formed steel lipped channels with optimum cross-sectional dimensions have been obtained depending on the profile thickness and design lengths of the structural member. In order to obtain optimum solutions for cross-sectional dimensions of the CFS lipped channel structural members which are independent from the design flexural lengths and profile thickness, searching for a compromise solution has been performed by exhaustive search method. The obtained cold-formed steel lipped channel structural members with optimum cross-sectional sizes have higher design buckling resistance under the axial compression at the same material consumption (stripe width) comparing with the cold-formed steel lipped channels proposed by the manufacturer. Web local buckling phenomenon has been occurred in all obtained CFS lipped channel cross-sections with optimum sizes.

**Keywords:** cold-formed steel, buckling resistance, torsional-flexural buckling, parametric optimization, exhaustive search method, compromise solution

**Introduction.** Previously, the use of cold-formed thin-walled profiles was limited to cases where reducing the weight of the structure was a priority, such as in the aviation or automotive industries. However, due to the development of production technology, corrosion protection, product availability as well as implementation of the design code the use of thin-walled structural elements, including cold-formed profiles is gradually expanding [1].

Today, various structural systems made from cold-formed steel (CFS) structural members used widely in the construction industry are imported intensively to the Ukrainian market of steel structures. Implementation of steel structures made from thin-walled cold-formed profiles in building practice is

relevant and economically reasonable. There are specific fields of application where their efficiency is the highest. However, the widespread application of the structures made from thin-walled cold-formed profiles of the domestic production is delayed due to the lack of domestic experience in economic and reliable design of such structures [1, 2].

**Literature review and problem statement.** In the papers [3] the authors said that “A high degree of flexibility in the manufacturing of various cross-sectional shapes provides a unique opportunity to further improve the load-carrying capacity of these structural elements through an optimization process, leading to more efficient and economical structural systems”. A brief review of optimization problem formulation, calculation techniques and algorithms, including gradient-based methods, stochastic search, artificial intelligent methods, and ant colony methods, have been discussed in the paper [4]. The optimization methodologies for CFS structural members have been also summarized and presented systematically in the paper [5, 6].

Lots of papers presented the results of shape optimization of cold-formed steel columns (see for example [7, 8, 9]). In the paper [10] the optimization problem formulation included fabrication and geometric enduse constraints. Shape optimization of manufacturable and usable cold-formed steel singly-symmetric and open columns has been also considered by the paper [11].

An optimization methodology intended to find the optimum cross-section sizes for CFS beam structural members with maximum flexural resistance has been provided by the paper [12]. Geometrical requirements according to EuroCode 3 as well as a number of manufacturing and practical constraints have been considered in scope of the optimization procedure. The flexural resistance of the CFS structural members has been determined based on the effective width approach regulated by EuroCode. The proposed optimization procedure has been performed based on the particle swarm optimization method.

In the paper [13] authors considered the optimal design problems for cold-formed steel lipped channel beams subjected to combined action of bending, shear, and web crippling. CFS beam structural member has been also considered by the papers [14, 15] where Big Bang-Big Crunch optimization and micro Genetic Algorithm have been used. In the paper [16] authors used the particle swarm optimization method in order to obtain optimum cross-section dimensions for lipped channels, folded-flanges, and super-sigma profiles used in modular building applications as beam structural members. Comparing to the conventional CFS sections the load-carrying flexural capacity of the structural members with optimum cross-sectional sizes has been improved significantly.

In the paper [3] a practical optimization methodology for the CFS beam-column structural members with different design lengths and thicknesses, subjected to various combinations of longitudinal force and bending moment has been proposed. The optimization procedure has been performed using a genetic algorithm, when the optimization problem has been formulated as maximization the buckling resistances of CFS structural members with

specified and constant material consumption.

The paper [17] presents an optimization procedure to obtain optimum dimensions for CFS channel cross-sections in structural members subjected to compression or bending. An optimization problem has been formulated as maximization of the load-carrying capacity and solved using genetic algorithms. Optimization has been performed for the different column design lengths taking into account the shift of the centroid of its effective cross-sections caused by the local buckling effects.

The paper [18] has been devoted to the shape optimization of cold-formed steel beam-columns with practical and manufacturing constraints. CFS beam-column structural member has been also considered by the papers [19, 20] in scope of unconstrained and constrained optimization procedures.

Particular attention has been paid to the optimal folding of the CFS structural members. In the paper [1] a parametric optimization problem for single edge fold size in CFS structural members subjected to axial compression has been considered. The purpose function and constraints of the mathematical model has been formulated as continuously differentiable functions, then the parametric optimization problems has been successfully solved using the gradient projection non-linear methods [21, 22].

The similar optimization problem has been also considered in the paper [23], where a genetic algorithm has been used with further improvement of the optimal decision based on the gradient descent method. As a result CFS structural member with optimal single edge folds have higher load-carrying capacity comparing to the original designs.

In order to increase the widespread application of the structures made from CFS profiles of the domestic production, effective national ranges of assortments of CFS profiles have to be developed. In this paper, CFS lipped channel structural members subjected to axial compression are considered as research object, which investigated for the searching for optimum cross-sectional dimensions. The following research tasks are formulated: to develop a mathematical model and a numerical technique to solve an optimization problem for cross-sectional sizes of CFS structural members; to perform numerical investigations in order to obtain optimal solutions for considered research object; to develop a guide for designers relating to the optimum material distribution in the cross-sections of the CFS structural members.

**The aim and objectives of the study.** In order to increase the widespread application of the structures made from CFS profiles of the domestic production, effective national ranges of assortments of CFS profiles have to be developed. In this paper, CFS lipped channel structural members subjected to axial compression are considered as research object, which investigated for the searching for optimum cross-sectional dimensions. The following research tasks are formulated: to develop a mathematical model and a numerical technique to solve an optimization problem for cross-sectional sizes of CFS structural members; to perform numerical investigations in order to obtain optimal solutions for considered research object.

**Material and methods.** Applied optimum design problems for structures in

some cases are formulated as parametric optimization problems, namely as searching problems for unknown structural parameters, which provide an extreme value of the specified purpose function in the feasible region defined by the specified constraints [24]. The mathematical model of the parametric optimization problems includes a set of design variables, an objective function, as well as constraints, which reflect generally non-linear dependences between them.

Let formulate a parametric optimization problem as follow: to find optimum values of cross-sectional sizes for CFS lipped channel structural members subjected to axial compression when the profile perimeter (strip width), profile thickness, steel properties as well as design lengths of the structural member are constant and specified in advance.

The formulated parametric optimization problem can be stated in the following mathematical terms: to find unknown structural parameters:

$$\vec{X} = \{X_i\}^T, \quad i = \overline{1, N_X}; \quad (1)$$

providing the maximum value of the determined objective function:

$$f^* = f(\vec{X}^*) = \max_{\vec{X} \in \mathfrak{S}} f(\vec{X}); \quad (2)$$

in feasible region (search space)  $\mathfrak{S}$  defined by the following system of constraints:

$$\Phi(\vec{X}) = \{\varphi_\eta(\vec{X}) \leq 0 \mid \eta = \overline{1, N_{IC}}\}; \quad (3)$$

where  $\vec{X}$  – vector of the design variables (unknown structural parameters);  $N_X$  – total number of the design variables;  $f, \varphi_\eta$  – continuous functions of the vector argument;  $\vec{X}^*$  – optimum solution (the vector of optimum values of the structural parameters);  $f^*$  – optimum value of the objective function;  $N_{IC}$  – number of constraints-inequalities  $\varphi_\eta(\vec{X})$ , which define a feasible region in the design space  $\mathfrak{S}$ .

Overall cross-section dimensions of a CFS lipped channel, namely web height  $h$ , flange width  $b$  and single edge fold length  $c$  (Fig. 1) are considered as *design variables*. Initial data for optimization are profile thickness  $t$ , internal bend radius  $r = 1.5t$ , material properties (base yield strength  $f_{yb}$  and modulus of elasticity  $E$ ), design length of the structural member corresponded to the flexural buckling modes  $l_{ef} = l_{ef,y} = l_{ef,z}$ . The torsional buckling length  $l_{ef,T}$  is equals to the flexural buckling length  $l_{ef,z}$ .

Let us introduce in the plane of thin-walled cross-section a Cartesian coordinate system  $y_C O z_C$  with the origin in the center of mass  $C$  of the section, the direction of the coordinate system axes  $y_C O z_C$  coincides with the direction of principle axes of inertia. Let us also describe the considered section of thin-walled bar by a set of sectional points

$\mathbf{P} = \{\mathbf{p}_j = \{y_j, z_j\} \mid j = \overline{0, n}\}$  ( $y_j$  and  $z_j$  are the coordinates of  $j^{\text{th}}$  sectional point in the coordinate system  $y_C O z_C$  introduced above) and by a set of sectional segments  $\mathbf{S} = \{\mathbf{s}_i = \{\mathbf{p}_{i-1}, \mathbf{p}_i\} \mid i = \overline{1, n}\}$ , which connect to adjacent sectional points, where  $n$  is quantity of the sectional segments and  $n+1$  is

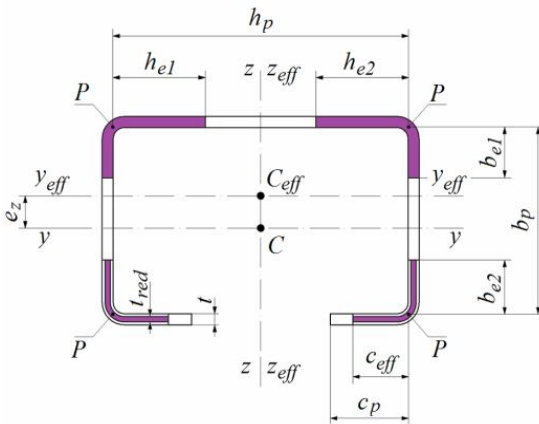


Fig. 1. Cross-section of the CFS lipped channel structural member

quantity of the sectional points. It should be noted that the coordinates of the sectional points depend on the design variables of the formulated optimization problem  $\mathbf{P} = \mathbf{P}(\bar{X})$ .

The following integral geometrical properties of considered cross-section can be calculated on the determined set  $\mathbf{P}$  of sectional points and set  $\mathbf{S}$  of sectional segments (see Annex C [25]):  $A_g$

is the gross cross-sectional area;  $I_y$ ,  $I_z$  are the second moments of inertia relative to the main axis of inertia, which coincide with the axes of global Cartesian coordinate system  $y_C O z_C$ ;  $i_y$ ,  $i_z$  are the radiuses of inertia relative to the main axis of inertia;  $I_\omega$  is the sectorial moment of inertia;  $I_t$  is the second moment of area for pure torsion. As the coordinates of the sectional points depend on the design variables, then the integral geometrical properties of the gross cross-section depends on the design variables as well.

Design sizes of plane cross-sectional elements (Fig. 1) for CFS lipped channel structural member are calculated according to [25] depending on the design variables  $h$ ,  $b$  and  $c$  as well as on the constant internal bend radius  $r$  and profile thickness  $t$  as presented below:

$$h_p = h - 2R + r_m \sqrt{2}; \quad (4)$$

$$b_p = b - 2R + r_m \sqrt{2}; \quad (5)$$

$$c_p = c - R + 0.5r_m \sqrt{2}; \quad (6)$$

where  $h_p$  – design web height;  $b_p$  – design flange width;  $c_p$  – single edge fold design length;  $r_m$  – middle bend radius,  $r_m = r + 0.5t$ ;  $R$  – external bend radius,  $R = r + t$ .

Relative slenderness  $\bar{\lambda}_{ph}$  of the web, relative slenderness  $\bar{\lambda}_{pb}$  of the flanges and relative slenderness  $\bar{\lambda}_{pc}$  of the single edge fold for CFS lipped channel are calculated according to [25, 26] as follow:

$$\bar{\lambda}_{ph} = \frac{h_p}{56,8t\varepsilon}; \quad (7)$$

$$\bar{\lambda}_{pb} = \frac{b_p}{56,8t\varepsilon}; \quad (8)$$

$$\bar{\lambda}_{pc} = \frac{c_p}{28,4t\varepsilon\sqrt{\tilde{\mathbf{k}}_{\sigma c}(c_p/b_p)}}; \quad (9)$$

where  $\varepsilon$  – material factor,  $\varepsilon = \sqrt{\frac{235}{f_{yb}[\text{MPa}]}}$ ;  $\tilde{\mathbf{k}}_{\sigma c}(c_p/b_p)$  – buckling factor calculated according to the dependency proposed by [25].

Cross-section flanges and web of CFS lipped channel structural member are subjected to post-buckling behavior (when local buckling occurs) in the case when its slenderness exceed limit value, namely web slenderness  $\bar{\lambda}_{ph} > 0,673$  and/or flange slenderness  $\bar{\lambda}_{pb} > 0,673$ . In this case effective widths of the web  $h_{eff}$  and flanges  $b_{eff}$  as well as effective cross-sectional sizes  $h_{e1}$ ,  $h_{e2}$ ,  $b_{e1}$ ,  $b_{e2}$  are defined according to [25, 26] as presented below:

– if  $\bar{\lambda}_{ph} > 0,673$ :

$$h_{e1} = h_{e2} = \frac{h_{eff}}{2} = \frac{h_p}{2\bar{\lambda}_{ph}} \left( 1 - \frac{0,22}{\bar{\lambda}_{ph}} \right) = 28,4t\varepsilon \left( 1 - \frac{12,496t\varepsilon}{h_p} \right); \quad (10)$$

– if  $\bar{\lambda}_{ph} \leq 0,673$ :

$$h_{e1} = h_{e2} = \frac{h_p}{2}; \quad (11)$$

– if  $\bar{\lambda}_{pb} > 0,673$ :

$$b_{e1} = \frac{b_{eff}}{2} = \frac{b_p}{2\bar{\lambda}_{pb}} \left( 1 - \frac{0,22}{\bar{\lambda}_{pb}} \right) = 28,4t\varepsilon \left( 1 - \frac{12,496t\varepsilon}{b_p} \right); \quad (12)$$

$$b_{e2} = \frac{b_{eff}}{2} = \frac{b_p}{2\bar{\lambda}_{pb}\sqrt{\chi_d}} \left( 1 - \frac{0,22}{\bar{\lambda}_{pb}\sqrt{\chi_d}} \right) = \frac{28,4t\varepsilon}{\sqrt{\chi_d}} \left( 1 - \frac{12,496t\varepsilon}{b_p\sqrt{\chi_d}} \right); \quad (13)$$

– if  $\bar{\lambda}_{pb} \leq 0,673$ :

$$b_{e1} = b_{e2} = \frac{b_p}{2}, \quad (14)$$

where  $\chi_d$  – reduction factor for the distortional buckling cross-section resistance calculated as presented below.

Single edge fold of CFS lipped channel cross-section is subjected to post-buckling behavior (when local buckling occurs) in case when its slenderness exceeds limit value ( $\bar{\lambda}_{pc} > 0,748$ ). In this case effective single edge fold width  $c_{eff}$  is determined according to [25] as follow:

– if  $\bar{\lambda}_{pc} > 0,748$  :

$$c_{eff} = \frac{28,4t\varepsilon}{\sqrt{\chi_d}} \sqrt{\tilde{k}_{\sigma c} \left( \frac{c_p}{b_p} \right)} \left( 1 - \frac{5,3392t\varepsilon}{c_p \sqrt{\chi_d}} \sqrt{\tilde{k}_{\sigma c} \left( \frac{c_p}{b_p} \right)} \right); \tag{15}$$

– if  $\bar{\lambda}_{pc} \leq 0,748$  :

$$c_{eff} = c_p. \tag{16}$$

Let us also describe the considered effective cross-section of thin-walled bar by a set of sectional points  $\mathbf{P}_{eff} = \left\{ \mathbf{p}_{eff,j} = \{y_{eff,j}, z_{eff,j}\} \mid j = \overline{0, n_{eff}} \right\}$  ( $y_{eff,j}$  and  $z_{eff,j}$  are the coordinates of  $j$  th sectional point in the coordinate system  $y_C O z_C$  introduced above) and by a set of sectional segments  $\mathbf{S}_{eff} = \left\{ \mathbf{s}_{eff,i} = \{ \mathbf{p}_{eff,i-1}, \mathbf{p}_{eff,i} \} \mid i = \overline{1, n_{eff}} \right\}$ , which connect to adjacent sectional points, where  $n_{eff}$  is quantity of the sectional segments and  $n_{eff} + 1$  is quantity of the sectional points. It should be noted that the coordinates of the sectional points depend on the design variables of the formulated optimization problem as well as on the effective cross-sectional sizes  $h_{e1}, h_{e2}, b_{e1}, b_{e2}, c_{eff}$  :

$$\mathbf{P}_{eff} = \mathbf{P}_{eff} (\bar{X}, h_{e1}, h_{e2}, b_{e1}, b_{e2}, c_{eff}).$$

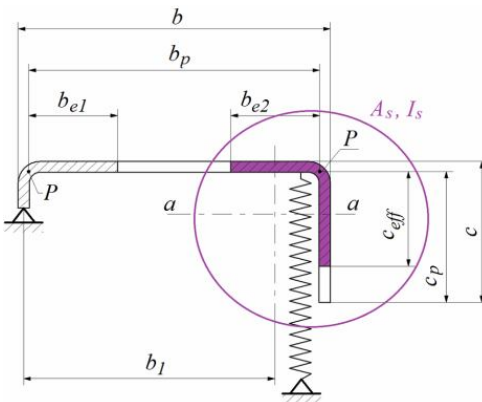


Fig. 2. Flange plane element of the CFS lipped channel stiffened by the single edge fold

The area  $A_{eff}$  of the effective cross-section of CFS lipped channel structural member subjected to axial compression can be calculated on the determined set  $\mathbf{P}_{eff}$  of sectional points and set  $\mathbf{S}_{eff}$  of sectional segments (see Annex C [25]). As the coordinates of the effective cross-sectional points depend on the design variables, then the area  $A_{eff}$  of the effective cross-section

of CFS lipped channel structural member subjected to compression depends on the design variables as well.

Single edge folds in CFS lipped channel structural members ensure partial restraint for plane flanges. In order to estimate such restraint, the design cross-section of the stiffener (Fig. 2) should be introduced into the further consideration. The design cross-section of the stiffener consists of single edge fold with effective width  $c_{eff}$  together with effective adjacent part of the flange with effective width  $b_{e2}$ . The thickness of the stiffener's design cross-section is equals to the profile thickness  $t$  in case when the distortional buckling does not occur ( $\chi_d = 1$ ). Otherwise, the reduced thickness  $t_{red}$  of the stiffener's design cross-section allowing for reduced stiffener resistance due to flexural buckling of the stiffener is determined according to [25] as follow:

$$t_{red} = \chi_d t. \quad (17)$$

Let us also describe the design cross-section of the stiffener by a set of sectional points  $\mathbf{P}_s = \{\mathbf{p}_{s,j} = \{y_{s,j}, z_{s,j}\} \mid j = \overline{0, n_s}\}$  ( $y_{s,j}$  and  $z_{s,j}$  are the coordinates of  $j$ th sectional point in the coordinate system  $y_c O z_c$  introduced above) and by a set of sectional segments  $\mathbf{S}_s = \{\mathbf{s}_{s,i} = \{\mathbf{p}_{s,i-1}, \mathbf{p}_{s,i}\} \mid i = \overline{1, n_s}\}$ , which connect to adjacent sectional points, where  $n_s$  is quantity of the sectional segments and  $n_s + 1$  is quantity of the sectional points. It should be noted that the coordinates of the sectional points depend on the design variables of the formulated optimization problem as well as on the effective cross-sectional sizes  $b_{e2}$ ,  $c_{eff}$  and reduced thickness  $t_{red}$ :

$$\mathbf{P}_s = \mathbf{P}_s(\bar{X}, b_{e2}, c_{eff}, t_{red}).$$

The following geometrical properties of the design cross-section of the stiffener can be calculated on the determined set  $\mathbf{P}_s$  of sectional points and set  $\mathbf{S}_s$  of sectional segments:  $A_s$  is the area of the stiffener's design cross-section;  $I_s$  is the second moment of inertia for the stiffener's design cross-section;  $b_{c,s}$  is the distance from the web-to-flange junction to the gravity center of the effective area of the edge stiffener.

The partial restraint for plane flanges provided by the single edge folds in CFS lipped channel structural members can be simulated using a linear spring. In case of the axial compression stiffness for such a linear spring can be estimated according to [25] as presented below:

$$K = \frac{E}{3,64} \cdot \frac{t^3}{b_{c,s}^2 (b_{c,s} + 1.5h - 3t)}. \quad (18)$$

It should be noted that analytical expression for stiffness of the linear spring presented above is restricted by the case of cold-formed structural members with flanges stiffened by single or double edge folds only and cross-section



symmetrical relatively to the main axes of inertia which is perpendicular to the web plane.

Then relative slenderness of the stiffener  $\bar{\lambda}_d$  corresponded to the flexural buckling of the stiffener is calculated according to [25] as follow:

$$\bar{\lambda}_d = \sqrt{\frac{f_{yb} A_s}{2 \sqrt{KEI_s}}} \quad (19)$$

The reduction factor  $\chi_d$  for the flexural buckling of the stiffener (or reduction factor for the distortional buckling cross-section resistance) is determined iteratively depending on relative slenderness  $\bar{\lambda}_d$  using dependency (5.12) proposed by [25]:

$$\chi_d = \Xi(\bar{\lambda}_d) \quad (20)$$

The maximization criterion of the minimum design buckling resistance of the structural member subjected to axial compression can be considered as the purpose function (2) of the optimization problem and can be written as follow:

$$N_{bRd, \min} = \min \{N_{byRd}, N_{bzRd}, N_{bT, Rd}, N_{bTF, Rd}\} \rightarrow \max ; \quad (21)$$

where  $N_{bRd, \min}$  – minimum design buckling resistance;  $N_{by, Rd}$ ,  $N_{bz, Rd}$  are the design buckling resistance for flexural buckling of the cold-formed structural member relative to the main axis of inertia  $y-y$  and  $z-z$  determined according to [25, 27];  $N_{bT, Rd}$ ,  $N_{bTF, Rd}$  are the design buckling resistance corresponded to the torsional and flexural-torsional buckling of the structural member calculated according to [25, 27].

Then the purpose function can be rewritten as follow:

$$N_{bRd, \min} = \frac{A_{eff} f_{yb}}{\gamma_{M1}} \times \min \{ \chi_y, \chi_z, \chi_T, \chi_{TF} \} \rightarrow \max ; \quad (22)$$

where  $\chi_y, \chi_z, \chi_T, \chi_{TF}$  – buckling factors allowing for the flexural buckling of the CFS structural member relative to the main axis of inertia  $y-y$  and  $z-z$ , as well as for the torsional and flexural-torsional buckling.

The buckling factors  $\chi_y, \chi_z, \chi_T, \chi_{TF}$  are determined from the relevant buckling curve  $b$  according to [25, 27] as:

$$\chi = \frac{1}{0.466 + 0.17\bar{\lambda} + 0.5\bar{\lambda}^2 + \sqrt{(0.466 - 0.83\bar{\lambda} + 0.5\bar{\lambda}^2)(0.466 + 1.17\bar{\lambda} + 0.5\bar{\lambda}^2)}}; \quad (23)$$

with substitution instead of  $\bar{\lambda}$  the relevant non-dimensional slendernesses  $\bar{\lambda}_y, \bar{\lambda}_z, \bar{\lambda}_T, \bar{\lambda}_{TF}$  corresponded to the considered buckling modes and calculated taking into account geometrical properties of the effective cross-section of the structural member subjected to the axial compression according to [25, 27] as presented below:

$$\bar{\lambda} = \sqrt{\frac{A_{eff} f_{yb}}{N_{cr}}}; \quad (24)$$

where  $N_{cr}$  – elastic critical force for the relevant buckling mode calculated depending on the design lengths and taking into account gross cross-section geometrical properties of the structural member and design lengths according to [27].

The non-dimensional slendernesses  $\bar{\lambda}_y$ ,  $\bar{\lambda}_z$ ,  $\bar{\lambda}_T$ ,  $\bar{\lambda}_{TF}$  are determined with substitution in (24) instead of  $N_{cr}$  the corresponded elastic critical force  $N_{cr,y}$ ,  $N_{cr,z}$ ,  $N_{cr,T}$  or  $N_{cr,TF}$ , here  $N_{cr,y}$  and  $N_{cr,z}$  are the elastic critical forces for the flexural buckling mode relative to the main axes of inertia  $y-y$  and  $z-z$  respectively;  $N_{cr,T}$ ,  $N_{cr,TF}$  are the elastic critical forces for the torsional and torsional-flexural buckling mode respectively.

System of constraints (3) for the formulated optimization problem consists of a constraint on the profile perimeter or on a strip width which can be written as presented below:

$$\frac{h+2b+2c}{P_{max}} - 1 \leq 0; \quad (25)$$

where  $P_{max}$  – maximum value of the cross-section perimeter for CFS lipped channel.

The constraints reflected design code requirements [25] for the ultimate slenderness of the cross-section elements of the CFS channel with flanges stiffened by single edge folds are also included in the system of constraints (3) and presented below:

$$\frac{h}{500t} - 1 \leq 0; \quad (26)$$

$$\frac{b}{60t} - 1 \leq 0; \quad (27)$$

$$\frac{c}{50t} - 1 \leq 0; \quad (28)$$

$$0.2 - \frac{c}{b} \leq 0; \quad (29)$$

$$\frac{c}{b} - 0.6 \leq 0. \quad (30)$$

Additionally, a constraint on the minimum gap between single edge folds ends allowing for providing an access to the internal surface of the CFS lipped channel (for example, in order to organize a bolted connection on the profile flanges [28, 29]) is included to the system of constraints (3) as well and written as below:

$$\frac{h-2c}{d_{min}} - 1 \leq 0; \quad (31)$$

where  $d_{min}$  is the minimum gap between single edge folds ends.

Thus, the optimization problem of cross-sectional sizes for CFS lipped channel structural member subjected to axial compression is formulated as follow: to find optimum cross-sectional sizes of CFS lipped channel (web height  $h$ , flange width  $b$  and single edge fold length  $c$ ) providing the maximum value of the determined objective function (21) in the feasible region defined by the system of constraints (25) –(31), when the profile perimeter (strip width), profile thickness, design lengths of the structural member as well as material properties are constant and specified in advance.

**Optimization results.** The following CFS lipped channels from the whole profile assortment range manufactured by the company «Blachy Pruszyński» [30] have been chosen to further optimization: C100×48×18 and C100×60×19. Other lipped channels have the same flange widths (48 mm and 60 mm) and have deeper web height simultaneously indicating their more rational usage as beam-column or beam structural members. The strip widths for the chosen CFS lipped channels are 23.2 cm and 25.8 cm respectively.

The following design flexural buckling length has been considered as initial data for optimization: 1.5 m, 2.0 m and 2.5 m. The use of single profiles for long-length CFS structural member with the design length greater than 2.5 m as well as short-length CFS structural members with the design length smaller than 1.5 m is not rational.

Taking into account small dimensionality the formulated parametric optimization problem has been solved by exhaustive search method using the software written in Python. As optimization results the CFS lipped channels with optimum cross-sectional dimensions have been obtained depending on the profile thickness and design lengths of the structural member. The obtained CFS lipped channel structural members with optimum cross-sectional sizes have higher design buckling resistance under the axial compression comparing with the CFS lipped channels with the same stripe width proposed by the manufacturer [30]. The increasing of the load-carrying capacity up to and including 12.14% (for the strip width 23.2 cm) and 19.01% (for the strip width 25.8 cm) has been achieved (Tab. 1 and Tab. 2).

Table 1  
CFS lipped channel structural members with optimum cross-sectional sizes  
(strip width is  $P_{max} = 23.2$  cm)

| Buckling length, m | $t$ , [cm] | Optimum cross-sectional sizes of the lipped channel, [cm] | $N_{brd, min}$ , [kN] | Buckling mode    | Web local buckling | Flange local buckling | Distorsional buckling | Load-carrying capacity increasing, % |
|--------------------|------------|---|-----------------------|------------------|--------------------|-----------------------|-----------------------|--------------------------------------|
| 1.5                | 0.100      | 8.8×4.5×2.7   | 31.696                | tors.-flex.      | Yes                | Yes                   | Yes                   | 12.14                                |
|                    | 0.125      | 8.8×4.5×2.7   | 41.871                | tors.-flex.      | Yes                | Yes                   | Yes                   | 10.81                                |
|                    | 0.150      | 8.8×4.5×2.7   | 51.664                | tors.-flex.      | Yes                | No                    | Yes                   | 9.65                                 |
|                    | 0.175      | 9.8×4.2×2.5   | 63.914                | tors.-flex.      | Yes                | No                    | No                    | 12.66                                |
|                    | 0.200      | 9.8×4.2×2.5   | 73.285                | tors.-flex.      | Yes                | No                    | No                    | 10.92                                |
|                    | 0.225      | 9.8×4.2×2.5   | 82.890                | tors.-flex.      | Yes                | No                    | No                    | 9.40                                 |
|                    | 0.250      | 9.6×4.3×2.5   | 92.140                | tors.-flex.      | Yes                | No                    | No                    | 5.55                                 |
|                    | 0.275      | 9.6×4.3×2.5   | 102.099               | flex. minor axis | Yes                | No                    | No                    | 5.88                                 |

| Buckling length, m | $t$ , [cm] | Optimum cross-sectional sizes of the lipped channel, [cm] | $N_{brd, min}$ , [kN] | Buckling mode    | Web local buckling | Flange local buckling | Distorsional buckling | Load-carrying capacity increasing, % |
|--------------------|------------|---|-----------------------|------------------|--------------------|-----------------------|-----------------------|--------------------------------------|
| 2.0                | 0.300      | 9.2×4.4×2.6   | 111.737               | tors.-flex.      | No                 | No                    | No                    | 3.37                                 |
|                    | 0.100      | 9.8×4.2×2.5   | 21.941                | tors.-flex.      | Yes                | Yes                   | Yes                   | 11.04                                |
|                    | 0.125      | 9.8×4.2×2.5   | 28.539                | tors.-flex.      | Yes                | Yes                   | Yes                   | 10.32                                |
|                    | 0.150      | 9.8×4.2×2.5   | 35.164                | tors.-flex.      | Yes                | No                    | Yes                   | 9.50                                 |
|                    | 0.175      | 9.8×4.2×2.5   | 43.189                | tors.-flex.      | Yes                | No                    | No                    | 11.35                                |
|                    | 0.200      | 9.6×4.3×2.5   | 49.898                | tors.-flex.      | Yes                | No                    | No                    | 9.38                                 |
|                    | 0.225      | 9.2×4.4×2.6   | 56.837                | tors.-flex.      | Yes                | No                    | No                    | 7.30                                 |
|                    | 0.250      | 9.2×4.4×2.6   | 64.433                | flex. minor axis | Yes                | No                    | No                    | 5.03                                 |
| 2.5                | 0.275      | 9.0×4.5×2.6   | 71.707                | tors.-flex.      | No                 | No                    | No                    | 3.04                                 |
|                    | 0.300      | 9.0×4.6×2.5   | 78.879                | flex. minor axis | No                 | No                    | No                    | 1.26                                 |
|                    | 0.100      | 9.8×4.2×2.5   | 15.699                | tors.-flex.      | Yes                | Yes                   | Yes                   | 10.72                                |
|                    | 0.125      | 9.8×4.2×2.5   | 20.445                | tors.-flex.      | Yes                | Yes                   | Yes                   | 10.11                                |
|                    | 0.150      | 9.8×4.2×2.5   | 25.446                | tors.-flex.      | Yes                | No                    | Yes                   | 9.39                                 |
|                    | 0.175      | 9.6×4.3×2.5   | 31.099                | tors.-flex.      | Yes                | No                    | No                    | 9.53                                 |
|                    | 0.200      | 9.2×4.4×2.6   | 36.385                | tors.-flex.      | Yes                | No                    | No                    | 7.22                                 |
|                    | 0.225      | 9.2×4.5×2.5   | 41.836                | flex. minor axis | Yes                | No                    | No                    | 4.39                                 |
| 2.0                | 0.250      | 9.4×4.7×2.2   | 47.263                | tors.-flex.      | Yes                | No                    | No                    | 1.18                                 |
|                    | 0.275      | 9.8×5.0×1.7   | 53.058                | tors.-flex.      | Yes                | No                    | No                    | 5.36                                 |
|                    | 0.300      | 9.2×5.0×2.0   | 59.257                | flex. minor axis | No                 | No                    | No                    | 9.68                                 |

Table 2

CFS lipped channel structural members with optimum cross-sectional sizes  
(strip width is  $P_{max} = 25.8$  cm)

| Buckling length, m | $t$ , [cm] | Optimum cross-sectional sizes of the lipped channel, [cm] | $N_{brd, min}$ , [kN] | Buckling mode    | Web local buckling | Flange local buckling | Distorsional buckling | Load-carrying capacity increasing, % |
|--------------------|------------|---|-----------------------|------------------|--------------------|-----------------------|-----------------------|--------------------------------------|
| 1.5                | 0.100      | 9.8×5.0×3.0   | 37.761                | tors.-flex.      | Yes                | Yes                   | Yes                   | 18.80                                |
|                    | 0.125      | 9.8×5.0×3.0   | 50.890                | tors.-flex.      | Yes                | Yes                   | Yes                   | 17.31                                |
|                    | 0.150      | 9.8×5.0×3.0   | 64.073                | tors.-flex.      | Yes                | Yes                   | Yes                   | 16.32                                |
|                    | 0.175      | 10.8×4.7×2.8  | 80.942                | tors.-flex.      | Yes                | No                    | No                    | 19.66                                |
|                    | 0.200      | 10.8×4.7×2.8  | 92.314                | tors.-flex.      | Yes                | No                    | No                    | 17.72                                |
|                    | 0.225      | 10.8×4.7×2.8  | 103.775               | tors.-flex.      | Yes                | No                    | No                    | 16.20                                |
|                    | 0.250      | 10.8×4.7×2.8  | 115.367               | tors.-flex.      | Yes                | No                    | No                    | 14.88                                |
|                    | 0.275      | 10.8×4.7×2.8  | 127.125               | tors.-flex.      | Yes                | No                    | No                    | 13.71                                |
| 2.0                | 0.300      | 10.8×4.7×2.8  | 139.079               | tors.-flex.      | Yes                | No                    | No                    | 12.83                                |
|                    | 0.100      | 9.8×5.0×3.0   | 27.611                | tors.-flex.      | Yes                | Yes                   | Yes                   | 18.71                                |
|                    | 0.125      | 10.8×4.7×2.8  | 36.181                | tors.-flex.      | Yes                | Yes                   | Yes                   | 17.97                                |
|                    | 0.150      | 10.8×4.7×2.8  | 44.738                | tors.-flex.      | Yes                | No                    | Yes                   | 17.22                                |
|                    | 0.175      | 11.4×4.5×2.7  | 55.376                | flex. minor axis | Yes                | No                    | No                    | 19.60                                |
|                    | 0.200      | 10.8×4.7×2.8  | 63.852                | tors.-flex.      | Yes                | No                    | No                    | 18.44                                |
|                    | 0.225      | 10.8×4.7×2.8  | 72.675                | tors.-flex.      | Yes                | No                    | No                    | 17.50                                |
|                    | 0.250      | 10.6×4.8×2.8  | 81.223                | tors.-flex.      | Yes                | No                    | No                    | 15.96                                |
| 2.0                | 0.275      | 10.6×4.8×2.8  | 90.040                | flex. minor axis | Yes                | No                    | No                    | 14.45                                |
|                    | 0.300      | 10.2×4.9×2.9  | 99.673                | tors.-flex.      | Yes                | No                    | No                    | 13.51                                |

| Buckling length, m | $t$ , [cm] | Optimum cross-sectional sizes of the lipped channel, [cm] | $N_{bRd, min}$ , [kN] | Buckling mode    | Web local buckling | Flange local buckling | Distorsional buckling | Load-carrying capacity increasing, % |
|--------------------|------------|---|-----------------------|------------------|--------------------|-----------------------|-----------------------|--------------------------------------|
| 2.5                | 0.100      | 10.8×4.7×2.8  | 20.192                | tors.-flex.      | Yes                | Yes                   | Yes                   | 19.01                                |
|                    | 0.125      | 10.8×4.7×2.8  | 26.228                | tors.-flex.      | Yes                | Yes                   | Yes                   | 18.53                                |
|                    | 0.150      | 10.8×4.7×2.8  | 32.448                | tors.-flex.      | Yes                | No                    | Yes                   | 17.96                                |
|                    | 0.175      | 10.8×4.7×2.8  | 39.897                | tors.-flex.      | Yes                | No                    | No                    | 19.40                                |
|                    | 0.200      | 10.8×4.7×2.8  | 46.532                | flex. minor axis | Yes                | No                    | No                    | 18.38                                |
|                    | 0.225      | 10.6×4.8×2.8  | 53.195                | flex. minor axis | Yes                | No                    | No                    | 16.85                                |
|                    | 0.250      | 10.2×4.9×2.9  | 60.157                | tors.-flex.      | Yes                | No                    | No                    | 15.22                                |
|                    | 0.275      | 10.0×5.0×2.9  | 67.017                | tors.-flex.      | Yes                | No                    | No                    | 12.97                                |
|                    | 0.300      | 10.0×5.1×2.8  | 74.037                | flex. minor axis | Yes                | No                    | No                    | 10.62                                |

Table 1 and Table 2 present the optimum cross-sectional sizes for CFS lipped channel structural members depending on the profile thickness as well as on the different design lengths corresponded to the flexural buckling modes. As you can see from the Table 1 and Table 2 the torsional-flexural buckling resistance of CFS lipped channel structural members has been determinative for the majority of the optimum decisions. Web local buckling phenomenon has been occurred in all obtained CFS lipped channel cross-sections with optimum sizes. Flange local buckling phenomenon as well as distortional buckling phenomenon has been occurred in obtained optimum CFS lipped channel cross-sections with small profile thicknesses only (up to and including 0.15 mm – for flange local buckling phenomenon and 0.175 mm – distortional buckling phenomenon).

In order to obtain optimum solutions for cross-sectional dimensions of the CFS lipped channel structural members which are independent from the design flexural lengths and profile thickness, searching for a compromise solution has been performed by exhaustive search method with the following criterion:

$$\sum_{l_{ef}} \left( \sum_t 1 - \frac{\mathfrak{N}_{bRd, min}(t, l_{ef})}{N_{bRd, min}} \right) \rightarrow \min ; \quad (32)$$

where  $N_{bRd, min}$  – minimum design buckling resistance of the lipped channel structural members with optimum cross-sectional sizes according to the Tables 1 and 2;  $\mathfrak{N}_{bRd, min}(t, l_{ef})$  – minimum design buckling resistance of the lipped channel structural members with “compromise” cross-sectional dimensions calculated depending on the profile thickness and flexural design length.

As optimization results there are two “compromise” solutions have been obtained: C88×45×27 (for the strip width 23.2 cm corresponded to the initial profile C100×48×18) and C98×50×30 (for the strip width 25.8 cm corresponded to the initial profile C100×60×19). The obtained CFS lipped channel structural members with „compromise” cross-sectional sizes have higher design buckling resistance under the axial compression comparing with the CFS lipped channels with the same stripe width proposed by the

manufacturer [30]. The increasing of the load-carrying capacity has been achieved in range 9.0...18.9% (for the strip width 25.8 cm) and up to and including 12.14% (for the strip width 23.2 cm) (Tab. 3 and Tab. 4).

Table 3

CFS lipped channel structural members with optimum cross-sectional sizes (strip width is  $P_{max} = 23.2$  cm corresponded to the initial profile C100×48×18)

| Buckling length, m | $t$ , [cm]  | Optimum cross-sectional sizes of the lipped channel, [cm] | $N_{bRd, min}$ , [kN] | Compromise solution, [cm] | $N_{bRd, min}$ , [kN] | Load-carrying capacity decreasing relating to the optimum solution, % | Load-carrying capacity increasing relating to the initial solution, % |
|--------------------|-------------|---|-----------------------|---------------------------|-----------------------|---|---|
| 1.5                | 0.100       | 8.8×4.5×2.7   | 31.696                | 8.8×4.5×2.7               | 31.696                | –   | 12.14   |
|                    | 0.125       | 8.8×4.5×2.7   | 41.871                |                           | 41.871                | –   | 10.81   |
|                    | 0.150       | 8.8×4.5×2.7   | 51.664                |                           | 51.664                | –   | 9.65  |
|                    | 0.175       | 9.8×4.2×2.5   | 63.914                |                           | 63.053                | 1.35  | 11.47   |
|                    | 0.200       | 9.8×4.2×2.5   | 73.285                |                           | 72.135                | 1.57  | 9.50  |
|                    | 0.225       | 9.8×4.2×2.5   | 82.890                |                           | 81.384                | 1.82  | 7.72  |
|                    | 0.250       | 9.6×4.3×2.5   | 92.140                |                           | 90.836                | 1.41  | 4.20  |
|                    | 0.275       | 9.6×4.3×2.5   | 102.099               |                           | 100.524               | 1.54  | 4.41  |
| 0.300              | 9.2×4.4×2.6 | 111.737   | 110.471               | 1.13                      | 2.26                  |   |   |
| 2.0                | 0.100       | 9.8×4.2×2.5   | 21.941                | 8.8×4.5×2.7               | 21.856                | 0.39  | 10.70   |
|                    | 0.125       | 9.8×4.2×2.5   | 28.539                |                           | 28.326                | 0.74  | 9.65  |
|                    | 0.150       | 9.8×4.2×2.5   | 35.164                |                           | 34.834                | 0.94  | 8.65  |
|                    | 0.175       | 9.8×4.2×2.5   | 43.189                |                           | 42.180                | 2.34  | 9.23  |
|                    | 0.200       | 9.6×4.3×2.5   | 49.898                |                           | 48.941                | 1.92  | 7.61  |
|                    | 0.225       | 9.2×4.4×2.6   | 56.837                |                           | 56.060                | 1.37  | 6.02  |
|                    | 0.250       | 9.2×4.4×2.6   | 64.433                |                           | 63.575                | 1.33  | 3.75  |
|                    | 0.275       | 9.0×4.5×2.6   | 71.707                |                           | 71.513                | 0.27  | 2.78  |
| 0.300              | 9.0×4.6×2.5 | 78.879  | 77.413                | 1.86                      | –0.62                 |   |   |
| 2.5                | 0.100       | 9.8×4.2×2.5   | 15.699                | 8.8×4.5×2.7               | 15.522                | 1.13  | 9.71  |
|                    | 0.125       | 9.8×4.2×2.5   | 20.445                |                           | 20.111                | 1.63  | 8.62  |
|                    | 0.150       | 9.8×4.2×2.5   | 25.446                |                           | 24.917                | 2.08  | 7.47  |
|                    | 0.175       | 9.6×4.3×2.5   | 31.099                |                           | 30.361                | 2.37  | 7.34  |
|                    | 0.200       | 9.2×4.4×2.6   | 36.385                |                           | 35.771                | 1.69  | 5.62  |
|                    | 0.225       | 9.2×4.5×2.5   | 41.836                |                           | 41.616                | 0.52  | 3.88  |
|                    | 0.250       | 9.4×4.7×2.2   | 47.263                |                           | 46.259                | 2.12  | –0.96   |
|                    | 0.275       | 9.8×5.0×1.7   | 53.058                |                           | 49.805                | 6.13  | –0.82   |
| 0.300              | 9.2×5.0×2.0 | 59.257  | 53.163                | 10.28                     | –0.67                 |   |   |

Table 4

CFS lipped channel structural members with optimum cross-sectional sizes (strip width is  $P_{max} = 25.8$  cm corresponded to the initial profile C100×60×19)

| Buckling length, m | $t$ , [cm] | Optimum cross-sectional sizes of the lipped channel, [cm] | $N_{bRd,min}$ [kN] | Compromise solution | $N_{bRd,min}$ [kN] | Load-carrying capacity decreasing relating to the optimum solution, % | Load-carrying capacity increasing relating to the initial solution, % |
|--------------------|------------|---|--------------------|---------------------|--------------------|---|---|
| 1.5                | 0.100      | 9.8×5.0×3.0   | 37.761             | 9.8×5.0×3.0         | 37.761             | –   | 18.80   |
|                    | 0.125      | 9.8×5.0×3.0   | 50.890             |                     | 50.890             | –   | 17.31   |
|                    | 0.150      | 9.8×5.0×3.0   | 64.073             |                     | 64.073             | –   | 16.32   |
|                    | 0.175      | 10.8×4.7×2.8  | 80.942             |                     | 80.182             | 0.94  | 18.90   |
|                    | 0.200      | 10.8×4.7×2.8  | 92.314             |                     | 91.342             | 1.05  | 16.85   |
|                    | 0.225      | 10.8×4.7×2.8  | 103.775            |                     | 102.548            | 1.18  | 15.20   |
|                    | 0.250      | 10.8×4.7×2.8  | 115.367            |                     | 113.834            | 1.33  | 13.74   |
|                    | 0.275      | 10.8×4.7×2.8  | 127.125            |                     | 125.231            | 1.49  | 12.40   |
|                    | 0.300      | 10.8×4.7×2.8  | 139.079            | 136.768             | 1.66               | 11.36   |   |
| 2.0                | 0.100      | 9.8×5.0×3.0   | 27.611             | 9.8×5.0×3.0         | 27.611             | –   | 18.71   |
|                    | 0.125      | 10.8×4.7×2.8  | 36.181             |                     | 36.085             | 0.26  | 17.76   |
|                    | 0.150      | 10.8×4.7×2.8  | 44.738             |                     | 44.646             | 0.20  | 17.05   |
|                    | 0.175      | 11.4×4.5×2.7  | 55.376             |                     | 54.463             | 1.65  | 18.25   |
|                    | 0.200      | 10.8×4.7×2.8  | 63.852             |                     | 62.643             | 1.89  | 16.86   |
|                    | 0.225      | 10.8×4.7×2.8  | 72.675             |                     | 71.084             | 2.19  | 15.65   |
|                    | 0.250      | 10.6×4.8×2.8  | 81.223             |                     | 79.830             | 1.72  | 14.49   |
|                    | 0.275      | 10.6×4.8×2.8  | 90.040             |                     | 88.914             | 1.25  | 13.36   |
|                    | 0.300      | 10.2×4.9×2.9  | 99.673             | 98.367              | 1.31               | 12.36   |   |
| 2.5                | 0.100      | 10.8×4.7×2.8  | 20.192             | 9.8×5.0×3.0         | 20.065             | 0.63  | 18.50   |
|                    | 0.125      | 10.8×4.7×2.8  | 26.228             |                     | 25.962             | 1.01  | 17.70   |
|                    | 0.150      | 10.8×4.7×2.8  | 32.448             |                     | 32.066             | 1.18  | 16.99   |
|                    | 0.175      | 10.8×4.7×2.8  | 39.897             |                     | 38.968             | 2.33  | 17.48   |
|                    | 0.200      | 10.8×4.7×2.8  | 46.532             |                     | 45.341             | 2.56  | 16.21   |
|                    | 0.225      | 10.6×4.8×2.8  | 53.195             |                     | 52.088             | 2.08  | 15.08   |
|                    | 0.250      | 10.2×4.9×2.9  | 60.157             |                     | 59.246             | 1.51  | 13.92   |
|                    | 0.275      | 10.0×5.0×2.9  | 67.017             |                     | 66.846             | 0.26  | 12.75   |
|                    | 0.300      | 10.0×5.1×2.8  | 74.037             | 72.718              | 1.78               | 9.00  |   |

**Discussion of results.** The optimum length of the single edge fold in all optimum CFS lipped channel cross-sections was greater comparing with the single edge fold length of CFS lipped channels proposed by the manufacturer. The average optimum ratio of the single edge fold length to the flange width  $c/b$  has been obtained as 0.58. The average optimum ratio of the flange width to the web height  $b/h$  has been received equal to 0.46. It should be noted, that the optimum ratio between the second moments of inertia relatively to the minor and major axis of inertia respectively has been received for all optimum solutions in range 0.2...0.29 due to the type of the cross-section and post-buckling behavior of the lipped channel web. The radiuses of inertia with respect to the main axes of inertia have been obtained for all CFS lipped

channel with optimum cross-sectional dimensions as follow:  
 $i_y = (0.38...0.39)h$ ,  $i_z = (0.37...0.41)b$ .

**Conclusion.** Searching for optimum cross-sectional sizes of CFS lipped channel structural members taking into account post-buckling behavior and structural requirements has been realized. The obtained CFS lipped channel structural members with optimum cross-sectional sizes have higher design buckling resistance under the axial compression comparing with the CFS lipped channels with the same stripe width proposed by the manufacturer.

The torsional-flexural buckling resistance of CFS lipped channel structural members has been determinative for the majority of the optimum decisions. Web local buckling phenomenon has been occurred in all obtained CFS lipped channel cross-sections with optimum sizes. The optimum length of the single edge fold in all optimum CFS lipped channel cross-sections was greater comparing with the single edge fold length of CFS lipped channels proposed by the manufacturer.

Presented results of the performed optimization calculation allow developing guides for designers relating to the optimum material distribution in the cross-sections of CFS structural members as well as are base to develop effective national ranges of assortments of cold-formed profiles.

#### REFERENCES

1. *Bilyk, S. I., Yurchenko, V. V.* Size optimization of single edge folds for cold-formed structural members // Strength of Materials and Theory of Structures: Scientific-and-technical collected articles. – 2020. – Iss. 105. – Pp. 73-86. doi: <http://doi.org/10.32347/2410-2547.2020.105.73-86>.
2. *Yurchenko, V.* Algorithm for shear flows in arbitrary cross-sections of thin-walled bars // Magazine of Civil Engineering. – 2019. – 192(8). – Pp. 3-26. DOI: <http://doi.org/10.18720/MCE.92.1>
3. *Mojtabaei, S. M., Becque, J., Hajirasouliha, I.* Structural size optimization of single and built-up cold-formed steel beam-column members // Journal of Structural Engineering. – 2021. – 147 (4). –No. 04021030. doi: [http://doi.org/10.1061/\(asce\)st.1943-541x.0002987](http://doi.org/10.1061/(asce)st.1943-541x.0002987).
4. *Leng, J.* Optimization Techniques for Structural Design of Cold-Formed Steel Structures // In Recent Trends in Cold-Formed Steel Construction.– Woodhead Publishing, Sawston, UK, 2016. – Pp. 129–151.
5. *Liang, H., Roy, K., Fang, Z., Lim, J. B. P.* A Critical Review on Optimization of Cold-Formed Steel Members for Better Structural and Thermal Performances // Buildings. – 2022.– 12, 34. doi: <http://doi.org/10.3390/buildings12010034>.
6. *Becque, J.* Optimization of cold-formed steel products: Achievements, challenges and opportunities // CE/PAPERS. – 2019.–3. – Pp. 211–218. doi: <http://doi.org/10.1002/cepa.1048>.
7. *Ammash, H. K.* Shape optimization of innovation cold-formed steel columns under uniaxial compressive loading // Jordan Journal of Civil Engineering. – 2017. – 11. – 3.
8. *Leng, J., Guest, J. K., Schafer, B. W.* Shape optimization of cold-formed steel columns // Thin-Walled Structures. – 2011. – 49. –Pp. 1492–1503. doi: <http://doi.org/10.1016/j.tws.2011.07.009>.
9. *Ye, J., Mojtabaei, S. M., Hajirasouliha, I.* Local-flexural interactive buckling of standard and optimised cold-formed steel columns // Journal of Constructional Steel Research. – 2018. – 144. – Pp. 106–118. doi: <http://doi.org/10.1016/j.jcsr.2018.01.012>.
10. *Leng, J., Li, Z., Guest, J. K., Schafer, B. W.* Shape optimization of cold-formed steel columns with fabrication and geometric enduse constraints // Thin-Walled Structures. – 2014. – 85. – Pp. 271–290. doi: <http://doi.org/10.1016/j.tws.2014.08.014>.



11. Wang, B., Gilbert, B. P., Guan, H., Teh, L. H. Shape optimisation of manufacturable and usable cold-formed steel singly-symmetric and open columns // *Thin-Walled Structures*. – 2016. – 109. – Pp. 271–284. doi: <http://doi.org/10.1016/j.tws.2016.10.004>
12. Ye, J., Hajirasouliha, I., Becque, J., Pilakoutas, K. Development of more efficient cold-formed steel channel sections in bending // *Thin-Walled Structures*. – 2016. – 101. – Pp. 1–13. doi: <http://doi.org/10.1016/j.tws.2015.12.021>.
13. Gatheeshgar, P., Poologanathan, K., Gunalan, S., Shyha, I., Tsavdaridis, K. D., Corradi, M. Optimal design of cold-formed steel lipped channel beams: Combined bending, shear, and web crippling // *Structures*. – 2020. – 28. – Pp. 825–836. doi: <http://doi.org/10.1016/j.istruc.2020.09.027>.
14. Lee, J., Kim, S. M., Park, H. S., Woo, B. H. Optimum design of cold-formed steel channel beams using micro Genetic Algorithm // *Engineering Structures*. – 2005. – 27. – Pp. 17–24. doi: <http://doi.org/10.1016/j.engstruct.2004.08.008>.
15. Mojtabaei, S. M., Ye, J., Hajirasouliha, I. Development of optimum cold-formed steel beams for serviceability and ultimate limit states using Big Bang-Big Crunch optimization // *Engineering Structures*. – 2019. – 195. – Pp. 172–181. doi: <http://doi.org/10.1016/j.engstruct.2019.05.089>.
16. Gatheeshgar, P., Poologanathan, K., Gunalan, S., Tsavdaridis, K. D., Nagaratnam, B., Iacovidou, E. Optimised cold-formed steel beams in modular building applications // *Journal of Building Engineering*. – 2020. – 32. – No. 101607. doi: <http://doi.org/10.1016/j.jobe.2020.101607>.
17. Ma, W., Becque, J., Hajirasouliha, I., Ye, J. Cross-sectional optimization of cold-formed steel channels to Eurocode 3 // *Engineering Structures*. – 2015. – 101. – Pp. 641–651. doi: <http://doi.org/10.1016/j.engstruct.2015.07.051>.
18. Parastesh, H., Hajirasouliha, I., Taji, H., Bagheri Sabbagh, A. Shape optimization of cold-formed steel beam-columns with practical and manufacturing constraints // *Journal of Constructional Steel Research*. – 2019. – 155. – Pp. 249–259. doi: <http://doi.org/10.1016/j.jcsr.2018.12.031>.
19. Wang, B., Bosco, G. L., Gilbert, B. P., Guan, H., Teh, L. H. Unconstrained shape optimisation of singly-symmetric and open cold-formed steel beams and beam-columns // *Thin-Walled Structures*. – 2016. – 104. – Pp. 54–61. doi: <http://doi.org/10.1016/j.tws.2016.03.007>.
20. Parastesh, H., M. Mojtabaei, S., Taji, H., Hajirasouliha, I., B. Sabbagh, A. Constrained optimization of anti-symmetric cold-formed steel beam-column sections // *Engineering Structures*. – 2021. – 228. – No. 111452. doi: <http://doi.org/10.1016/j.engstruct.2020.111452>.
21. Peleshko, I. D., Yurchenko, V. V. Parametric Optimization of Metallic Rod Constructions with using the Modified Method of Gradient Projection // *International Applied Mechanics*. – 2021. – Vol. 57. – No. 4. – Pp. 78–95. doi: <http://doi.org/10.1007/s10778-021-01096-0>.
22. Yurchenko, V., Peleshko, I. Methodology for solving parametric optimization problems of steel structures // *Magazine of Civil Engineering*. – 2021. – 107(7). – Article No. 10705. doi: <http://doi.org/10.34910/MCE.107.5>
23. Moharrami, M., Louhghalam, A., Tootkaboni, M. Optimal folding of cold formed steel cross sections under compression // *Thin-Walled Structures*. – 2014. – 76. – Pp. 145–156.
24. Permyakov, V. O., Yurchenko, V. V., Peleshko, I. D. An optimum structural computer-aided design using hybrid genetic algorithm // *Proceeding of the International Conference Progress in Steel, Composite and Aluminium Structures*. – Taylor & Francis Group, London, 2006. – Pp. 819–826.
25. EN 1993-1-3:2006: EuroCode 3: Design of steel structures - Part 1-3: General rules – Supplementary rules for cold-formed members and sheeting.
26. EN 1993-1-5:2006: EuroCode 3: Design of steel structures - Part 1-5: General rules – Plated structural elements.
27. EN 1993-1-1:2005: EuroCode 3: Design of steel structures - Part 1-1: General rules and rules for buildings.
28. Perelmuter, A., Kriksunov, E., Gavrilenko, I., Yurchenko, V. Designing bolted end-plate connections in compliance with Eurocode and Ukrainian codes: consistency and contradictions // *Selected papers of the 10<sup>th</sup> International Conference “Modern Building Materials, Structures and Techniques”*. – 2010. – Vol. II. – Pp. 733–743.
29. Karpilovsky, V. S., Kriksunov, E. Z., Perelmuter, A. V., Yurchenko, V. V. Analysis and design

of steel structural joints and connection: software implementation // International Journal for Computational Civil and Structural Engineering. – 2021. – Vol. 17. – Is. 2. – Pp. 58–66. doi: <http://doi.org/10.22337/2587-9618-2021-17-2-58-66>.

30. Assortment ranges of the cold-formed profiles for light gauge steel structures of the Ukrainian manufacturers. UCSC-014-16, 2016. 32 p., (ukr).

*Стаття надійшла 26.09.2022*

*Юрченко В.В., Пелешко І.Д.*

### **ПОШУК КОМПРОМІСНОГО РОЗВ'ЯЗКУ В ЗАДАЧАХ ОПТИМІЗАЦІЇ РОЗМІРІВ ПОПЕРЕЧНИХ ПЕРЕРІЗІВ ЕЛЕМЕНТІВ КОНСТРУКЦІЙ ІЗ ХОЛОДНОГНУТИХ ПРОФІЛІВ**

У статті розглядається задача параметричної оптимізації розмірів поперечних перерізів для стержневих елементів конструкцій із С-подібних холодногнутих профілів, які підлягають дії поздовжнього стиску. Задача оптимізації сформульована як задача пошуку оптимальних розмірів перерізів стержневих елементів конструкцій з врахуванням їх закритичної роботи (втрати місцевої стійкості стінки та полиць та/або втрати стійкості форми перерізу), а також конструктивних вимог за умов, що периметр профілю (ширина штрипси), товщина профілю, розрахункові довжини стержневого елемента конструкції та механічні характеристики сталі приймалися постійними та наперед заданими. Як критерій оптимальності розглядалася максимізація несучої здатності елемента конструкції на втрату загальної стійкості. Сформульована задача оптимізації розв'язана за допомогою методу вичерпного пошуку з використанням програмного забезпечення, розробленого мовою Python. Як результат були отримані холодногнуті С-подібні профілі з оптимальними розмірами поперечного перерізу залежно від товщини профілю та розрахункових довжин стержневого елемента конструкції. З метою отримання оптимальних розмірів поперечних перерізів С-подібних холодногнутих профілів, що не залежатимуть від розрахункових довжин і товщини профіля, здійснено пошук компромісного розв'язку. Отримані холодногнуті С-подібні профілі з оптимальними розмірами поперечних перерізів характеризуються високою несучою здатністю на втрату загальної стійкості при осьовому стиснанні при тій самій витраті сталі (ширини штрипси) порівняно з С-подібними холодногнутими профілями, що пропонуються виробником профілів. Для усіх оптимальних розв'язків характерним є явище втрати місцевої стійкості стінки профіля.

**Ключові слова:** холодногнута сталь, несуча здатність щодо втрати стійкості, згинально-крутильне випучування, параметрична оптимізація, метод вичерпного пошуку, компромісний розв'язок.

*Yurchenko V.V., Peleshko I.D.*

### **SEARCHING FOR A COMPROMISE SOLUTION IN CROSS-SECTION SIZE OPTIMIZATION PROBLEMS OF COLD-FORMED STEEL STRUCTURAL MEMBERS**

A parametric optimization problem of cross-sectional sizes for cold-formed steel lipped channel structural members subjected to axial compression has been considered by the paper. An optimization problem is formulated as to define optimum cross-sectional sizes of cold-formed structural member taking into account post-buckling behavior (web and flange local and distortional buckling) of the member as well as structural requirements when the profile perimeter (strip width), profile thickness, design lengths of the structural member as well as material properties are constant and specified in advance. Maximization of the load-carrying capacity of the cold-formed structural member has been assumed as purpose function. The formulated parametric optimization problem has been solved by exhaustive search method using the software written in Python. As optimization results the cold-formed steel lipped channels with optimum cross-sectional dimensions have been obtained depending on the profile thickness and design lengths of the structural member. In order to obtain optimum solutions for cross-sectional dimensions of the CFS lipped channel structural members which are independent from the design flexural lengths and profile thickness, searching for a compromise solution has been performed by exhaustive search method. The obtained cold-formed steel lipped channel structural members with optimum cross-sectional sizes have higher design buckling resistance under the axial compression at the same material consumption (strip width) comparing with the cold-formed steel lipped channels

proposed by the manufacturer. Web local buckling phenomenon has been occurred in all obtained CFS lipped channel cross-sections with optimum sizes.

**Keywords:** cold-formed steel, buckling resistance, torsional-flexural buckling, parametric optimization, exhaustive search method, compromise solution.

*Юрченко В.В., Пелешко І.Д.*

### **ПОИСК КОМПРОМИССНОГО РЕШЕНИЯ В ЗАДАЧАХ ОПТИМИЗАЦИИ РАЗМЕРОВ ПОПЕРЕЧНЫХ СЕЧЕНИЙ ЭЛЕМЕНТОВ КОНСТРУКЦИЙ ИЗ ХОЛОДНОГНУТЫХ ПРОФИЛЕЙ**

В статье рассматривается задача параметрической оптимизации размеров поперечных сечений для стержневых элементов конструкций из С-образных холодногнутых профилей, подлежащих действию продольного сжатия. Задача оптимизации сформулирована как задача поиска оптимальных размеров сечений стержневых элементов конструкций с учетом их закрытической работы (потери местной устойчивости стенки и полохи/илипотери устойчивости формы сечения), а также конструктивных требований при условии, что периметр профиля (ширина штрипсы), толщина профиля, расчетные длины стержневого элемента конструкции механические характеристики стали принимались постоянными наперед заданными. В качестве критерия оптимальности рассматривалась максимизация несущей способности элемента конструкции на потерю общей устойчивости. Сформулированная задача оптимизации решена при помощи метода ищущего поиска с использованием программного обеспечения, разработанного на языке Python. В качестве результатов были получены холодногнутые С-образные профили оптимальными размерами поперечных сечений в зависимости от толщины профиля и расчетных длин стержневого элемента конструкции. С целью получения оптимальных размеров поперечных сечений С-образных холодногнутых профилей, не зависящих от расчетных длин и толщины профиля, реализован поиск компромиссного решения. Полученные холодногнутые С-образные профили оптимальными размерами поперечных сечений характеризуются большей несущей способностью на потерю общей устойчивости при продольном сжатии при том же расходе стали (ширине штрипсы) по сравнению с С-образными холодногнутыми профилями, предлагаемыми изготовителем профилей. Для всех оптимальных решений характерно явление потери местной устойчивости стенки профиля.

**Ключевые слова:** холодногнутая сталь, несущая способность относительно потери устойчивости, изгибно-крутильное выпучивание, параметрическая оптимизация, метод ищущего поиска, компромиссное решение

УДК 624.04.012.4.044, 519.853

*Юрченко В.В., Пелешко І.Д.* **Пошук компромісного розв'язку в задачах оптимізації розмірів поперечних перерізів елементів конструкцій з холодногнутих профілів** // Опір матеріалів і теорія споруд: наук.-тех. збірн. – К.: КНУБА, 2022. – Вип. 109. – С. 72-92.

*У статті розглядається задача пошуку оптимальних розмірів перерізів стержневих елементів конструкцій з врахуванням їх закритичної роботи (втрати місцевої стійкості стінки та полиць та/або втрати стійкості форми перерізу), а також конструктивних вимог за умов, що периметр профіля (ширина штрипси), товщина профіля, розрахункові довжини стержневого елемента конструкції та механічні характеристики сталі приймалися постійними та наперед заданими. Як критерій оптимальності розглядалася максимізація несучої здатності елемента конструкції на втрату загальної стійкості. Як результат були отримані холодногнуті С-подібні профілі з оптимальними розмірами поперечного перерізу залежно від товщини профіля та розрахункових довжин стержневого елемента конструкції. З метою отримання оптимальних розмірів поперечних перерізів С-подібних холодногнутих профілів, що не залежатимуть від розрахункових довжин і товщини профіля, здійснено пошук компромісного розв'язку. Отримані холодногнуті С-подібні профілі з оптимальними розмірами поперечних перерізів характеризуються вищою несучою здатністю на втрату загальної стійкості при осьовому стисканні при тій самій витраті сталі порівняно з С-подібними холодногнутими профілями, що пропонуються виробником профілів.*

Іл. 2. Табл. 4. Бібліог. 30 назв.

УДК 624.04.012.4.044, 519.853

*Yurchenko V.V., Peleshko I.D. Searching for a compromise solution in cross-section size optimization problems of cold-formed steel structural members // Strength of Materials and Theory of Structures: Scientific-and-technical collected articles – Kyiv: KNUBA, 2022. – Issue 109. – P. 72-92.*

*The paper considers a searching problem for optimum cross-sectional sizes of cold-formed structural member taking into account post-buckling behavior (web and flange local and distortional buckling) of the member as well as structural requirements when the profile perimeter (strip width), profile thickness, design lengths of the structural member as well as material properties are constant and specified in advance. Maximization of the load-carrying capacity of the cold-formed structural member has been assumed as purpose function. As optimization results the cold-formed steel lipped channels with optimum cross-sectional dimensions have been obtained depending on the profile thickness and design lengths of the structural member. In order to obtain optimum solutions for cross-sectional dimensions of the cold-formed lipped channel structural members which are independent from the design flexural lengths and profile thickness, searching for a compromise solution has been performed by exhaustive search method. The obtained cold-formed steel lipped channel structural members with optimum cross-sectional sizes have higher design buckling resistance under the axial compression at the same material consumption (strip width) comparing with the cold-formed steel lipped channels proposed by the manufacturer.*

*Figs. 2. Tabs. 4. Refs. 30.*

УДК624.04.012.4.044, 519.853

*Юрченко В. В., Пелешко И. Д. Поиск компромиссного решения в задачах оптимизации размеров поперечных сечений элементов конструкций из холодногнутой профилей // Сопроотивление материалов и теория сооружений: науч.- тех. сборн. – К.: КНУСА, 2022. – Вып. 109. – С. 72-92.*

*В статье рассматривается задача поиска оптимальных размеров сечений стержневых элементов конструкций с учетом их критической работы (потери местной устойчивости стенки и пололки/или потери устойчивости формы сечения), а также конструктивных требований при условии, что периметр профиля (ширина штрипсы), толщина профиля, расчетные длины стержневого элемента конструкции и механические характеристики стали принимались постоянными наперед заданными. В качестве критерия оптимальности рассматривалась максимизация несущей способности элемента конструкции на потерю общей устойчивости. В качестве результатов были получены холодногнутые С-образные профили оптимальными размерами поперечных сечений в зависимости от толщины профиля и расчетных длин стержневого элемента конструкции. С целью получения оптимальных размеров поперечных сечений С-образных холодногнутых профилей, не зависящих от расчетных длин и толщины профиля, реализован поиск компромиссного решения. Полученные холодногнутые С-образные профили оптимальными размерами поперечных сечений характеризуются большей несущей способностью на потерю общей устойчивости при продольном сжатии при том же расходе стали (ширине штрипсы) по сравнению с С-образными холодногнутыми профилями, предлагаемыми изготовителем профилей.*

*Ил. 2. Табл. 4. Библиог. 30 назв.*

**Автор:(вчена ступень, вчене звання, посада):** доктор технічних наук, професор кафедри металевих та дерев'яних конструкцій ЮРЧЕНКО Віталіна Віталіївна.

**Адреса робоча:** 03680 Україна, м. Київ, Повітрофлотський пр., 31, Київський національний університет будівництва і архітектури.

**Роб. тел.:** +38(044)249-71-91

**Моб. тел.:** +38(063)89-26-491

**E-mail:** vitalina@scadsoft.com

**SCOPUS ID:** 25637856200

**ORCID ID:** <https://orcid.org/0000-0003-4513-809X>

**Автор:(вчена ступень, вчене звання, посада):** кандидат технічних наук, доцент кафедри будівельного виробництва ПЕЛЕШКО Іван Дмитрович.

**Адреса робоча:** 79013 Україна, м. Львів, вул. Ст. Бандери 12, Національний університет «Львівська політехніка»

**Роб. тел.:** +38 (032) 258-25-41

**Моб. тел.:** +38(098)41-57-517

**E-mail:** [ipeleshko@polynet.lviv.ua](mailto:ipeleshko@polynet.lviv.ua)

**SCOPUS ID:** 25637832500

**ORCID ID:** <https://orcid.org/0000-0001-7028-9653>